



SYMPOSIUM

Attention and Motivated Response to Simulated Male Advertisement Call Activates Forebrain Dopaminergic and Social Decision-Making Network Nuclei in Female Midshipman Fish

Paul M. Forlano,^{*,†,‡,§,¶,1} Roshney R. Licorish,^{*} Zachary N. Ghahramani,^{*,†} Miky Timothy,^{*} Melissa Ferrari,^{||} William C. Palmer[#] and Joseph A. Sisneros^{#,**}

^{*}Department of Biology, Brooklyn College, The City University of New York, Brooklyn, NY, USA; [†]Biology Subprogram in Ecology, Evolutionary Biology, and Behavior, The Graduate Center, City University of New York, New York, NY, USA; [‡]Biology Subprogram in Neuroscience, The Graduate Center, City University of New York, New York, NY, USA; [§]Psychology Subprogram in Behavioral and Cognitive Neuroscience, The Graduate Center, City University of New York, New York, NY, USA; [¶]Aquatic Research and Environmental Assessment Center, Brooklyn College, Brooklyn, NY, USA; ^{||}Edward R. Murrow High School, Brooklyn, NY, USA; [#]Department of Psychology, University of Washington, Seattle, WA, USA; ^{**}Virginia Bloedel Hearing Research Center, Seattle, WA, USA

From the symposium “Integrating Cognitive, Motivational and Sensory Biases Underlying Acoustic and Multimodal Mate Choice” presented at the annual meeting of the Society for Integrative and Comparative Biology, January 4–8, 2017 at New Orleans, Louisiana.

¹E-mail: pforlano@brooklyn.cuny.edu

Synopsis Little is known regarding the coordination of audition with decision-making and subsequent motor responses that initiate social behavior including mate localization during courtship. Using the midshipman fish model, we tested the hypothesis that the time spent by females attending and responding to the advertisement call is correlated with the activation of a specific subset of catecholaminergic (CA) and social decision-making network (SDM) nuclei underlying auditory-driven sexual motivation. In addition, we quantified the relationship of neural activation between CA and SDM nuclei in all responders with the goal of providing a map of functional connectivity of the circuitry underlying a motivated state responsive to acoustic cues during mate localization. In order to make a baseline qualitative comparison of this functional brain map to unmotivated females, we made a similar correlative comparison of brain activation in females who were unresponsive to the advertisement call playback. Our results support an important role for dopaminergic neurons in the periventricular posterior tuberculum and ventral thalamus, putative A11 and A13 tetrapod homologues, respectively, as well as the posterior parvocellular preoptic area and dorsomedial telencephalon, (laterobasal amygdala homologue) in auditory attention and appetitive sexual behavior in fishes. These findings may also offer insights into the function of these highly conserved nuclei in the context of auditory-driven reproductive social behavior across vertebrates.

Introduction

Socially motivated behavior related to sexual reproduction is indicative of an individual's fine-tuned, physiologically regulated internal state which is simultaneously receptive and responsive to conspecific sensory cues. Vocal-acoustic social communication is fundamental for reproduction in several vertebrate groups and is thought to have first evolved in teleost fishes (Bass et al. 2008). In order to respond

appropriately to a male advertisement or “mate” call the receiver must be able to (1) detect and encode signals with context-dependent salience and (2) respond and attend to the signal in a motivated manner adaptive for reproduction. Investigations of these various processing mechanisms by receiver systems have received recent attention in songbirds, amphibians and fishes (for reviews see Wilczynski and Ryan 2010; Hoke and Pitts 2012; Maney 2013;

Forlano et al. 2015b; Maney and Rodriguez-Saltos 2016). However, there is still little known regarding the coordination of auditory responsiveness with decision-making and subsequent motor responses that initiate social behavior including mate localization during courtship behavior.

The social decision-making network (SDM) proposed by O'Connell and Hofmann (2011, 2012) combines the mesolimbic reward system with the evolutionarily conserved social behavior network (SBN), a reciprocally connected group of hormone-sensitive nuclei in the basal forebrain and midbrain that is essential for basic behaviors expressed by all vertebrates which include maternal, sexual, aggressive, and communicative (Newman 1999; Goodson 2005; Goodson and Kabelik 2009; Goodson and Kingsbury 2013). An important component of the SDM is the ascending dopaminergic system which is thought to interact with the SBN to mediate appropriate behavioral responses to social cues (O'Connell and Hofmann 2011). While the idea of the SDM as a functional network across all vertebrate groups is largely theoretical, it does offer many hypotheses to test, especially in anamniotes (Goodson and Kingsbury 2013). Furthermore, dopamine has been shown to play important roles in appetitive female sexual behavior in a variety of vertebrates (Endepols et al. 2004; Ritters et al. 2007; Graham and Pfaus 2012; McHenry et al. 2017). Notably, songbirds provide some evidence that the salience of conspecific vocal signals can be modulated by steroid hormones via dopamine and noradrenaline (Caras 2013; Maney 2013). Although many dopaminergic cell populations exist within the forebrain of vertebrates (Yamamoto and Vernier 2011), with few exceptions (e.g., Bharati and Goodson 2006; O'Connell et al. 2013; Kelly and Goodson 2015), most studies have focused on the midbrain ventral tegmental area (VTA), (the major source of ascending dopaminergic input to forebrain limbic areas in mammals) in the context of social behavior. Therefore, significant insight into the role of forebrain dopamine groups in vertebrate social behavior can be gained by investigations across taxa and in a variety of social contexts. These studies are especially necessary in anamniotes such as teleost fishes where a direct homology to the mammalian VTA is unclear or absent and where other forebrain dopamine groups may confer functional equivalence to the VTA in social contexts (Tay et al. 2011; Goodson and Kingsbury 2013).

The plainfin midshipman fish, *Porichthys notatus*, is a highly appropriate model to address the above questions related to the neural basis underlying

female auditory-driven social behavior in vertebrates as the perception of the male advertisement call and the subsequent female phonotactic response to the social signal is essential to this species' reproduction (Bass and McKibben 2003; Sisneros 2009; Forlano et al. 2015b). Plainfin midshipman spawn in the late spring and early summer months in the rocky intertidal zone of northern California and Washington State in the United States. Males excavate and defend nests under rocks and court females at night with a long duration advertisement call, or hum. Females use the hum to locate a potential mate, deposit her eggs in the courting male's nest, and then return to deep waters offshore, while the nest-guarding male provides all the parental care for the offspring (Brantley and Bass 1994; Bass 1996; Bass and McKibben 2003; Forlano et al. 2015b). Only gravid females (ripe with eggs) exhibit robust unconditioned positive phonotaxis, a directed locomotor response toward (and subsequent localization of) the sound source produced by the "humming" male, and the fundamental frequency of the hum (approximately 100 Hz at 16 °C) has been shown to be necessary and sufficient to elicit this positive appetitive sexual behavior (McKibben and Bass 1998; Zeddies et al. 2010). Phonotaxis behavior in midshipman can be viewed as an unambiguous measure of arousal and motivation, with the female making a decision to respond to a salient social signal in an appropriate fashion (Forlano and Bass 2011). While only gravid females exhibit phonotaxis (spent females, who have released all their eggs, do not), there can be significant variation in responsiveness of gravid females, ranging from 30 to 70% in previous experiments (Zeddies et al. 2010). Once a female has localized the source of the hum playback, the duration of attending the speaker is also variable (but has not been systematically studied) and is the main focus of this paper. Therefore this simple behavior offers an excellent opportunity to test the hypothesis that SDM components are active in this social context during mate localization.

Importantly, recent studies in midshipman have also established a strong neuroanatomical foundation for catecholamines, and dopamine in particular, as modulators of seasonally plastic audition and auditory-driven social behavior (Forlano and Sisneros 2016). We recently identified dopaminergic neurons in the diencephalic periventricular posterior tuberculum (TPp) that directly innervate the sacculle, the main endorgan of hearing in midshipman and the site of seasonal, steroid-driven changes in auditory frequency sensitivity that allow for better encoding

of the male advertisement call (Forlano et al. 2014; Forlano et al. 2015b; Sisneros et al. 2004a). This same population of dopaminergic neurons directly innervates the auditory efferent nucleus (Perelmuter and Forlano 2017) and innervation of both areas varies seasonally depending on reproductive state (Forlano et al. 2015a). Tpp dopaminergic neurons appear to innervate the auditory thalamus, and several nodes of the SBN, including the periaqueductal gray (PAG) and basal forebrain areas (Forlano et al. 2014). Interestingly, Tpp dopamine neurons also project to the spinal cord and therefore are ideal candidate neurons to integrate sensory-motor and higher decision making processes (O'Connell and Hofmann 2011; Tay et al. 2011; Forlano et al. 2014). While several lines of evidence suggest that these neurons are homologous to mammalian A11 dopamine neurons (see Yamamoto and Vernier 2011; Schweitzer et al. 2012; Goodson and Kingsbury 2013; Forlano et al. 2014), they, along with other forebrain dopamine neurons may confer functions analogous to A10 dopamine neurons in the tetrapod VTA (Yamamoto and Vernier 2011; Goodson and Kingsbury 2013). Importantly, Tpp dopaminergic neurons and noradrenergic neurons of the locus coeruleus are active (via double labeling with cFos, an immediate early gene product and proxy for neural activity) in males exposed to playbacks of the hum and are therefore involved in processing acoustic social signals in this species (Petersen et al. 2013).

In order to test the hypothesis that the time spent by females attending to the advertisement call is correlated with the activation of a specific subset of catecholaminergic (CA) and SDM nuclei (Table 1) underlying auditory-driven sexual motivation, we utilized double-label immunofluorescence (-ir) histochemistry for cFos and tyrosine hydroxylase (TH), markers of neural activity and catecholamine synthesis, respectively. In addition, we quantified the relationship of neural activation between CA and SDM nuclei in all responders (females that displayed phonotaxis behavior) with the goal of providing a map of functional connectivity of the circuitry underlying the response to acoustic cues during mate localization. In order to make a baseline qualitative comparison of this functional brain map to unmotivated females, we made a similar correlative comparison of brain activation in females who were unresponsive to the advertisement call playback. Our results support an important role for two forebrain dopaminergic and two SDM nuclei in auditory attention and appetitive sexual behavior in vertebrates.

Materials and methods

Animals

All experimental animal procedures performed in this study were approved by the Institute for Animal Care and Use Committee of the University of California, Davis and CUNY Brooklyn College. During the late spring and summer breeding period, reproductively-primed, gravid (body cavity full of large, yolked eggs) females can be characterized by several factors which included high (>10%) gonadosomatic index (GSI, the ratio of gonad weight to total body weight), location collected (shallow intertidal zones as opposed to deep offshore sites), and the display of mate seeking behaviors (Sisneros et al. 2004b). Female midshipman fish were collected from nests by hand during the early morning low tide in the seasonal reproductive period (late May-June) in Tomales Bay near Marshall, California, USA. Females were transported in coolers with aerated sea water to the UC Davis Bodega Marine Laboratory (BML) where they were then group-housed with other females in aquaria with ambient temperature (11–16 °C) flow-through seawater until the phonotaxis behavioral assays were conducted after nightfall on the same day of collection. Based on GSI measurement all females used in this study were characterized as “gravid” upon sacrifice (see below).

Behavioral phonotaxis assay and brain (tissue) collection

Phonotaxis trials were conducted similar to that described in Zeddies et al. (2010). Prior to testing, individual females were held outside near the testing area in plastic 5 gallon buckets with water from the test tank and allowed to acclimate for 30 min. Trials were run in an outdoor cylindrical concrete tank (4 m in diameter, 0.75m in depth, water depth, 50 cm) after nightfall (21:00–2:00 h) since midshipman are nocturnal breeders. An underwater speaker suspended from a beam in the center of the tank was used to playback a pure tone that simulated the fundamental frequency of the male mate call, which was determined by ambient temperature each night (see McKibben and Bass 1998). A 30 cm diameter cylindrical mesh cage with openings at its base was placed 109 cm from the speaker where the playback sound was calibrated to 130 dB re: 1 μ Pa. With the sound playing continuously, fish were manually placed into the cylinder and allowed to swim toward the speaker at their own accord. The response times of the females recorded were based on the length of time that the female spent attending the speaker once she reached the source of the sound ($n = 12$).

Table 1 Catecholaminergic (TH-ir), social decision-making network (SDM), and auditory nuclei matched with corresponding putative mammalian homologues

Brain area	Putative mammalian homologue
TH-ir	
Vd	Striatum/basal ganglia ^{9,11,17,20}
Vp	Extended central amygdala/bed nucleus of stria terminalis ^{2,7,9,13}
PPa	A12 ²¹
VM-VL	A13 ^{18,21}
TPp	A11 ^{18,21}
LC	Locus coeruleus ^{15,18}
SDM/Auditory	
Dm ^a	Laterobasal amygdala ^{1,2,9,14,16,19,20}
Vv ^{a,b}	Septum ^{2,7,9,13,20}
Vd	Striatum/basal ganglia ^{9,11,17,20}
Vs ^{a,b}	Extended central amygdala/bed nucleus of stria terminalis ^{2,7,9,13}
Vp ^a	Extended central amygdala/bed nucleus of stria terminalis ^{2,7,9,13}
PPa ^{a,b}	POA ^{6,10}
PPp ^{a,b}	POA ^{6,10}
PM ^b	Paraventricular nucleus ^{4,5,8}
AT ^{a,b}	Ventromedial hypothalamus (in part) ^{3,6,7}
CPc ^a	Medial geniculate nucleus ¹²
PAG ^{a,b}	Periaqueductal/central gray ^{6,7}

Note: ^aConfirmed to receive auditory input in midshipman fish (Bass et al. 2000; Goodson and Bass 2002).

^bComponents of the social behavior network (SBN) as described for Osteichthyes (Goodson 2005).

¹(Braford 1995).

²(Bruce and Braford 2009).

³(Forlano et al. 2005).

⁴(Forlano and Cone 2007).

⁵(Gilchriest et al. 2000).

⁶(Goodson 2005).

⁷(Goodson and Kingsbury 2013).

⁸(Kapsimali et al. 2001).

⁹(Maximino et al. 2013).

¹⁰(Moore and Lowry 1998).

¹¹(Mueller and Wullmann 2009).

¹²(Mueller 2012).

¹³(Northcutt 1995).

¹⁴(Northcutt 2006).

¹⁵(Smeets and Gonzalez 2000).

¹⁶(Portavella et al. 2004).

¹⁷(Rink and Wullmann 2001).

¹⁸(Tay et al. 2011).

¹⁹(Von Trotha et al. 2014).

²⁰(Wullmann and Mueller 2004).

²¹(Yamamoto and Vernier 2011).

The latencies for positive response initiation are generally very short and were not recorded in this study. Each trial ended when the fish left the speaker and touched the wall of the tank; fish were then placed

back into the 5 gal holding tank for 2 h for cFos to accumulate (see Petersen et al. 2013) after which fish were deeply anesthetized by immersion in mixture of 0.025% benzocaine and sea water, weighed, measured, and then transcardially perfused with ice cold teleost ringers solution followed by 4% paraformaldehyde in 0.1 M phosphate buffer (PB; pH 7.2). Brains were then surgically removed and post fixed for 1 h in same fixative before storage at 4 °C in a 0.1 PB, 0.03% sodium azide solution. Ovaries were removed, weighed and GSI calculated at this time. The brains were then transported to CUNY Brooklyn College where they were cryoprotected in 30% sucrose PB solution for 24–48 h before they were sectioned via cryostat at 25 µm, in 2 series, in the transverse plane and collected onto positively charged superfrost slides then stored at – 80°C until they were immunohistochemically processed. In addition, a group of control animals ($n = 6$) which did not exhibit phonotaxis, were allowed to stay in the tank for 10–15 min, and like responders, were placed in individual buckets for 2 h, sacrificed and processed as above.

Immunohistochemistry

Fluorescence IHC was slightly modified from a previous protocol (Petersen et al. 2013). Slides were allowed to warm to room temperature prior to being washed 2 X 10 min in 0.1 M phosphate-buffered saline (PBS; pH 7.2), followed by a 1-h soak in blocking solution (PBS + 10% normal donkey serum + 0.3% Triton X-100; PBS-DS-T). After blocking, tissue was incubated for 18 h at room temperature in PBST-DS containing mouse anti-TH (1:1000; Millipore, Temecula, CA, USA) and rabbit anti-cFos (1:2000; sc-253 lot #C2510, Santa Cruz Biotechnology, Santa Cruz, CA, USA) primary antibodies. After incubation, slides were washed 5 X 10 min in PBS + 0.5% normal donkey serum (PBS-DS), followed by a 2-h incubation in PBS-DS-T combined with anti-mouse and anti-rabbit secondary antibodies conjugated to Alexa Fluor 488 and 568, respectively (1:200; Life Technologies, Norwalk, CT, USA). Slides were then washed 3 X 10 min in PBS, coverslipped with ProlongGold containing DAPI nuclear stain (Life Technologies).

Image acquisition and anatomy

Immunofluorescent images were acquired using an Olympus BX61 epifluorescence compound microscope using MetaMorph imaging and processing software. Each brain nucleus was captured with a 20× objective lens at the same exposure time and light

level. Each photomicrograph was obtained consecutively using Texas Red (Tx-Red), green fluorescence protein (GFP) and DAPI filter sets with a z-stack of seven levels each having a thickness of 1 μm . These photomicrographs were then combined into a single projected image with ImageJ (NIH, USA) using the “maximum intensity” z-projection function, and regions of interest (ROIs) were drawn after acquisition using DAPI to define neuroanatomical boundaries and outline cytoarchitecture. Sampling strategies were determined per region to account for intrinsic variation in size between brain areas. For unilateral sampling, the left side of the brain was imaged. In the case of tissue loss or damage, the opposite side of the brain was used or the section was omitted.

Figure images were level adjusted for accurate background compensation in GNU Image Manipulation Program (GIMP), merged from multiple micrographs, when necessary, in Adobe Photoshop CS5 (Adobe Systems, San Jose, CA) and organized, labeled, and formatted into final figures with Adobe Illustrator and GIMP.

Catecholaminergic nuclei of interest included the periventricular posterior tuberculum (TPp), locus coeruleus (LC), anterior parvocellular preoptic nucleus (PPa), ventromedial and ventrolateral thalamic nuclei (VM-VL), and the postcommissural (Vp) and dorsal (Vd) nuclei of the ventral telencephalon. All 6 of these nuclei were analyzed for %TH-ir neurons that contained cFos-ir, meaning all TH-ir neurons were counted and then the percentage of those TH-ir neurons that also contained cFos in their nucleus were counted to calculate %TH + cFos-ir. PPa, Vp, and Vd are nuclei that contain TH-ir neurons at their lateral boundary and in the latter two these neurons arguably lie just outside the boundaries defined by Nissl staining (Forlano et al. 2014); therefore in these areas cFos was also counted within the typically defined and more ventricular boundaries separately from where TH-ir neurons are located (see below). The measure of %TH + cFos was never combined with cFos alone in regions without TH neurons. Sampling of the LC and TPp were carried out as previously described (Petersen et al. 2013; Forlano et al. 2015a; Ghahramani et al. 2015) for an average of 11.3 (± 1.5 SD) and 9.1 (± 1.4 SD) sections per animal through the LC and TPp, respectively. Sampling of TH-ir neurons within PPa was carried out as described (Forlano et al. 2015a; Ghahramani et al. 2015) for an average of 12.2 ± 2.7 sections per animal. Sampling of VM-VL began rostral to CPC with the appearance of small, round TH-ir neurons lateral to the midline which form a continuous caudal chain converging at the

midline near the third ventricle (Forlano et al. 2014). TH-ir neurons in VM-VL were analyzed an average of 8 (± 1.3 SD) sections per animal. With the exception of the rostral extent of the nucleus (where it was necessary to take two images to capture all visible TH-ir neurons), a single image of each section was taken. Sampling of Vp started rostral to VM-VL, being a distinct cluster of cells positioned dorsomedial to the POA with TH-ir neurons arranged in the lateral aspect of the nucleus. TH-ir neurons in Vp were imaged an average of 7.3 (± 1.7 SD) sections per animal. The transition from Vp to Vd is based on the distinct appearance of the anterior commissure (ac) at the ventral base of the midline, dorsolateral to PPa. TH-ir neurons in Vd were sampled an average of 10 (± 2.3 SD) sections, stopping with the appearance of the olfactory bulbs.

Nuclei that were analyzed for presence of cFos-ir exclusive of TH-ir activity included the periaqueductal grey (PAG), compact division of the auditory thalamus (CPC), anterior tuberal nucleus of the hypothalamus (AT), preoptic nuclei (magnocellular, PM; posterior parvocellular, PPp; PPa), ventral telencephalic nuclei (Vp; Vd; supracommissural, Vs; ventral, Vv), and medial zone of the dorsal telencephalon (Dm; i.e., dorsomedial telencephalon). The PAG appears as a dense layer of cell bodies ventral to the cerebral aqueduct and medial to the periventricular cell layer of the torus semicircularis (Goodson and Bass 2002; Kittelberger and Bass 2013). Sampling of the PAG was carried out as previously described (Ghahramani et al. 2015). Images were taken across an average of 7.5 (± 1.4 SD) sections per animal. cFos-ir cells were quantified within the ROI that was drawn around the layer of cells comprising the PAG, lying ventral to the cerebral aqueduct. Sampling of CPC was carried out as described (Petersen et al. 2013; Forlano et al. 2015a), beginning with the DAPI-labeled wing-shaped band of cells lateral to the midline. A boundary was drawn around CPC, and cFos-ir cells were quantified within. CPC was sampled an average of 6.7 (± 1.2 SD) sections per animal. The AT was sampled as previously described (Petersen et al. 2013; Forlano et al. 2015a; Ghahramani et al. 2015), for an average of 3.1 (± 0.5 SD) and cFos-ir cells were quantified within the field of view ($143,139 \mu\text{m}^2$).

Three subregions of the POA were identified as per previously defined morphological features (Braford and Northcutt 1983; Goodson et al. 2003) and were analyzed for cFos-ir exclusive of TH-ir. These nodes were sampled based on their appearance in the brain moving rostrally: magnocellular division of the preoptic area (PM; 3.8 ± 1.6 SD sections sampled), posterior parvocellular preoptic nucleus (PPp;

2.9 \pm 1.2 SD), and PPa (4.3 \pm 1.7 SD). Note that since PM and Pp are sometimes found in the same section, cell counts for those regions were performed separately based on cytoarchitectural criteria but at times in shared sections.

Within the ventral telencephalon, we quantified cFos-ir exclusive of TH-ir across an average of 7.2 (\pm 2 SD) sections per animal through Vp and 9.3 (\pm 1.7 SD) sections through Vd. Both of these areas were sampled in a manner similar to the aforementioned TH-ir neuron sampling method, except images were taken at the midline since TH-ir neurons are largely found only at the lateral boundaries of each nucleus. Both Vs and Vv are oriented in close proximity to Vp and Vd, and do not contain TH-ir neurons. Sampling of Vs started with the appearance of the ac and rostral to the POA, where a single photomicrograph was taken so that the nucleus took up the field of view with the midline serving as the lateral boundary and ac serving as the ventral boundary of the image. Vv appears rostral to Vs and caudal to the olfactory bulbs (Forlano et al. 2014). Similar to Vs, sampling of Vv began with a single photomicrograph positioned at the midline so that Vv took up the field of view, and ended with the appearance of the olfactory bulbs. Images were taken across an average of 6.9 (\pm 1.9 SD) sections through Vs and 3 (\pm 0.7 SD) through Vv, and cFos-ir cells were quantified within the field of view (143,139 μm^2).

The location of the Dm has been thoroughly delineated in midshipman (Brantley and Bass 1988) and its precise neuroanatomical boundaries, chemoarchitecture, and sensitivity to cFos assay have recently been described in detail in zebrafish (Von Trotha et al. 2014). We unilaterally sampled serial sections from the core of the rostral Dm averaging 9.3 (\pm 1.0 SD) sections per animal. The lateral, inclusive boundary of Dm was defined by a seam of relatively dense DAPI staining running from a periventricular sulcus at the dorsal boundary of the brain ventrally to core of the telencephalic parenchyma. The entirety of the transverse extent of Dm was analyzed in selected sections, thus necessitating the imaging of two adjacent micrographs—a medial image bordering the telencephalic ventricle, and a lateral image containing the aforementioned sulcus and adjacent cellular density.

Quantitative analysis of catecholaminergic activity and cFos induction

Cell counts in the aforementioned TH-ir nuclei were done in accordance with prior studies (Petersen et al.

2013; Forlano et al. 2015a; Ghahramani et al. 2015). Experimenters were blind to the treatment conditions of any slides analyzed. Activation of CA neurons was measured by the occurrence of a cFos-ir nucleus within a TH-ir neuron, which we refer to herein as colocalization (Bharati and Goodson 2006; Petersen et al. 2013). To analyze the percentage of TH-ir neurons colocalized with cFos-ir, photomicrographs were taken under the same conditions as those used for analysis in the aforementioned auditory and SBN nuclei. Photomicrographs were combined into a single projected image with ImageJ. The GFP and DAPI channels were overlaid, and TH-ir neurons were counted manually. Individual TH-ir neurons were counted only if the perimeter of the cell was clearly outlined with a labeled neurite in addition to having a nucleus that exhibited colocalization with DAPI. The Tx-Red channel was then overlaid, and each instance where a TH-ir neuron had cFos-ir localized within the nucleus was counted. The sum of TH-ir neurons containing cFos-ir was divided by the total number of TH-ir neurons \times 100 for a percentage of TH + cFos-ir colocalization per brain region.

DAPI-labeled cell nuclei containing cFos signal in areas not containing TH-ir was accomplished through user interaction with a custom-written macro in ImageJ. Nuclei positive for cFos appear as distinct circles of relatively uniform bright signal that correspond to a distribution of points, corresponding to maximal peaks of label in an image. To assist with the detection of cells, observers first ran the “find maxima” algorithm after setting tolerance levels appropriate for the relative signal density and intensity of the given sample of tissue. Validity of automated cFos signal identification was confirmed visually after signal thresholding which was performed to account for relative fluorescence background and corrected as needed. The mean number of cFos-ir cells per section (total number of cFos-ir neurons divided by number of sections sampled) were computed per brain region in each animal.

Statistics

Statistical analyses were conducted using GraphPad Prism 6 software. Pearson correlations were performed between response time and %TH-ir + cFos-ir in Vp, Vd, PPa, VM-VL, Tpp, and LC, as well as cFos-ir/section in Dm, Vv, Vs, Vd, Vp, PPa, Pp, PM, AT, CPc, and PAG. Mann-Whitney U-tests were used to compare morphometrics between responding and nonresponding females due to uneven sample sizes between groups. To compare patterns of

brain activation between divergent states of behavior (responders vs. nonresponders), data were pooled for all nuclei sampled, and two separate correlation matrices were computed. Corrections for multiple comparisons within the same dataset were done by controlling for the false discovery rate (FDR) using the Benjamini-Hochberg procedure with an FDR of 0.25 (Butler and Maruska 2016). All significant *P*-values remained significant after correction; therefore, only the exact *P*-values and effect size (e.g., *r*-values) are included in each table. Statistics are reported herein as mean \pm standard deviation (SD) unless otherwise indicated.

Results

Morphometrics

As expected, female midshipman captured in the intertidal zone during the summer reproductive months had a high GSI (>10%). The GSI of responding females ($N=12$) ranged from 15.8–43.2% (mean = 32.8 ± 7.3 SD). Body mass ranged between 26.1–70.6 g (37.4 ± 12 SD), gonad mass ranged 4.2–21.3 g (9.4 ± 4.3 SD), and standard length (SL) ranged from 12.5–16.7 cm (13.7 ± 1.1 SD). In the group of nonresponding females ($N=6$), GSI ranged from 17.9–34.3% (26.6 ± 5.3 SD). Body mass ranged between 19.6–36 g (29.3 ± 7.6 SD), gonad mass ranged 3–8 g (6.2 ± 2.1 SD), and SL ranged from 11.7–14.3 cm (13.2 ± 1.1 SD). The amount of time responding females spent attending to the underwater speaker ranged from 4–14 min (7.3 ± 3.1 SD). There were no significant relationships between GSI and %TH + cFos-ir in any CA-ergic nuclei sampled. However, within responders, there were significant negative correlations between GSI and cFos-ir/section in Vd ($r_{10} = -0.656$, $P = 0.0206$), and cFos-ir/section in PPa within nonresponders ($r_{10} = -0.815$, $P = 0.048$).

Relationship between time attending and responding to speaker and cFos induction

Figs. 1 and 2 show representative micrographs of all brain areas sampled and measured for cFos induction, including 5 dopaminergic nuclei: Tpp (Fig. 1A and B), VM-VL (Fig. 1D and E), Vd (Fig. 2A), Vp (Fig. 2D), PPa (Fig. 2E), the noradrenergic LC (Fig. 2J); SBN/SDM nuclei: preoptic area subdivisions Ppp (Fig. 1G and H), PPa (Fig. 2E) PM (Fig. 2F), Dm (Fig. 1J and K), Vd (Fig. 2A), Vs (Fig. 2B), Vv (Fig. 2C), Vp (Fig. 2D), AT (Fig. 2H), PAG (Fig. 2I), and the auditory thalamus, CP, (Fig. 2G). Out of these areas, there were significant relationships between time attending speaker

and %TH + cFos-ir in VM-VL ($r_{10}^2 = 0.6444$, $P = 0.0017$) and Tpp ($r_{10}^2 = 0.526$, $P = 0.0076$), as well as cFos-ir/section in Dm ($r_{10}^2 = 0.5884$, $P = 0.0036$), and Ppp ($r_{10}^2 = 0.3678$, $P = 0.0365$). Fig. 1 shows correlation plots of cFos induction vs. time attending to the playback speaker of these four areas and representative sections from low (4–5 min) and high (10–11 min) responders. Importantly, unlike responders, nonresponders while subjected to the stimulus for varying lengths of time, showed no relationship of cFos-ir and time of exposure to the playback.

Brain activation correlations of responders and nonresponders

In an attempt to resolve functional relationships between TH-ir nuclei, SDM nodes, and auditory circuitry that may underlie divergent motivational states, correlation matrices were computed across all sampled brain regions within responders and within nonresponders (Fig. 3, Suppl. Table 1). There was a notable difference in the number of significant correlations between responders (18) and nonresponders (8). The only relationship that was consistent between the two behavioral states is the negative correlation between cFos-ir/section in Vp and Dm, being stronger in nonresponders ($r = -0.9931$, $P = 0.0069$) than responders ($r = -0.6059$, $P = 0.0368$).

Preoptic area

Interestingly, nonresponders showed no significant correlations involving preoptic nuclei. However, within responders, cFos-ir/section in Ppp and PM exhibited positive relationships with %TH + cFos-ir in both VM-VL ($r = 0.7059$, $P = 0.0103$) and Vd ($r = 0.7244$, $P = 0.0077$), respectively. %TH + cFos-ir in PPa was co-active with Vd ($r = 0.5899$, $P = 0.0435$) and Tpp ($r = 0.631$, $P = 0.0278$), and PPa cFos-ir/section was co-active with both Ppp ($r = 0.6603$, $P = 0.0194$) and CPc ($r = 0.7956$, $P = 0.002$).

Positive coactivation between multiple dopaminergic nuclei

In contrast with nonresponders, responding females showed notable coactivation amongst the majority of dopaminergic TH-ir nuclei sampled: %TH + cFos-ir in Vd was correlated with PPa ($r = 0.5899$, $P = 0.0435$) and VM-VL ($r = 0.5905$, $P = 0.0432$), and %TH + cFos-ir in Tpp was similarly correlated with PPa ($r = 0.631$, $P = 0.0278$) and VM-VL ($r = 0.8143$, $P = 0.0013$).

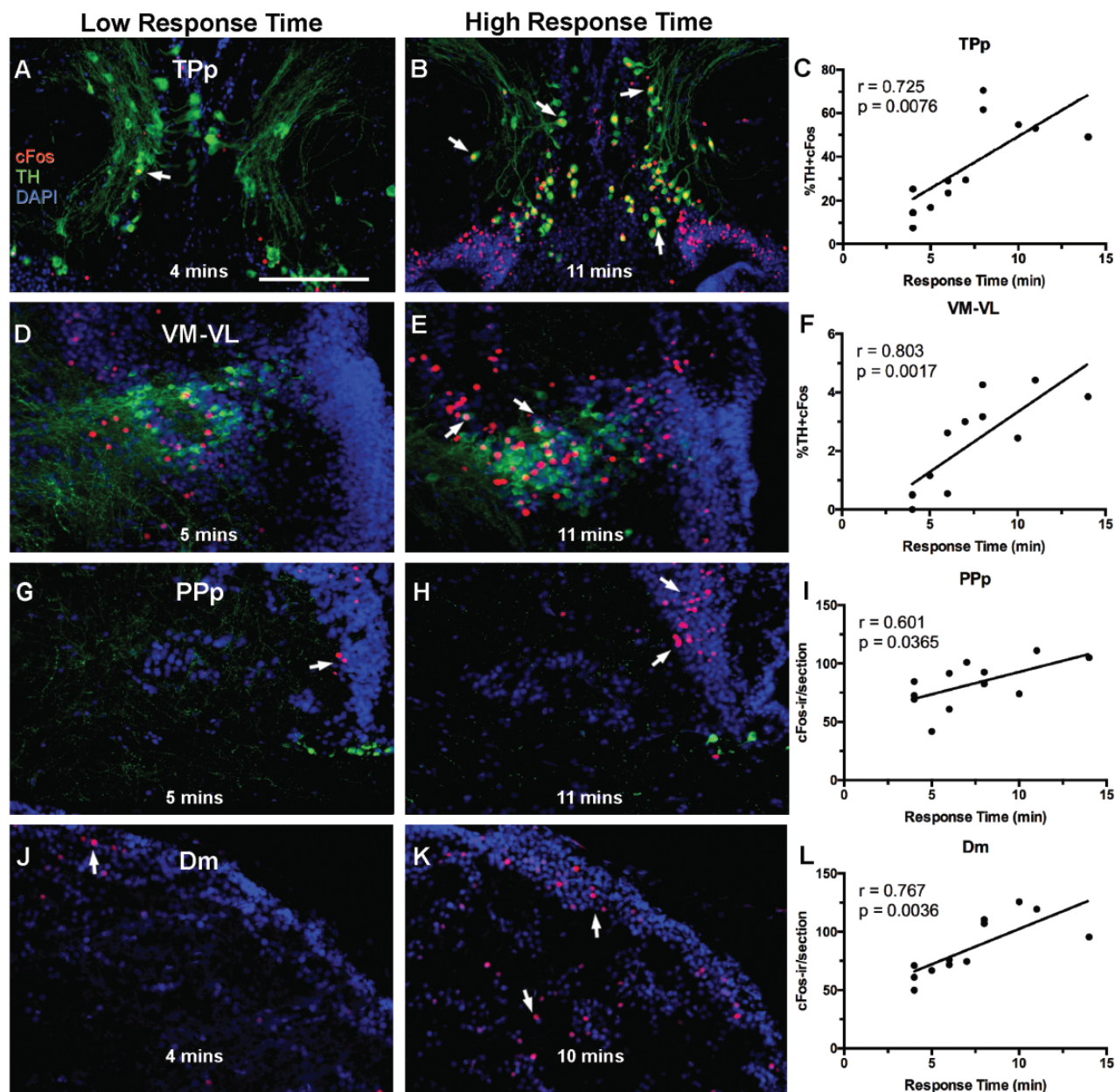


Fig. 1 Example micrographs showing nuclei found to have a significant relationship between time attending speaker and TH-ir + cFos colocalization (A–F) or cFos expression (G–L) in transverse sections. Graphed representation of data ($n = 12$) and Pearson's correlation results are presented for each region (C, F, I, L). Arrows in A–E indicate cFos-ir colocalized to TH-ir nuclei. (A–C) Periventricular posterior tuberculum (TPp): mean % colocalization of cFos in TH-ir cells is $36.28\% \pm 5.94\%$. (D–E) Ventromedial and ventrolateral nuclei of the thalamus (VM-VL): mean % colocalization of cFos in TH-ir cells in VM-VL is $2.2\% \pm 1.6\%$. (G–I) Posterior parvocellular preoptic nucleus (PPp) mean number of cFos cells per section is 82.21 ± 19.8 . (J–L) Medial zone of the dorsal telencephalon (Dm): number of cFos cells per section in Dm is 85.8 ± 24.8 . Arrows in G–K indicate Fos-ir within areas of interest. Scale bar = 100 μm .

TH-ir and SDM network interactions

In responders, Dm cFos-ir activity shared positive correlations with %TH + cFos-ir nuclei: PPA ($r = 0.5791$, $P = 0.0485$), VM-VL ($r = 0.7836$, $P = 0.0026$), and TPp ($r = 0.9273$, $P < 0.0001$). Nonresponders showed no relationships between cFos-ir activity in Dm with any TH-ir nuclei sampled. %TH + cFos-ir in VM-VL was also differentially

co-active between the two behavioral states: within responders, %TH + cFos-ir in VM-VL was correlated with cFos-ir/section in PPp ($r = 0.7059$, $P = 0.0103$), while in nonresponders it was correlated with cFos-ir/section in CPc ($r = 0.8116$, $P = 0.0499$). CPc in turn, in nonresponders, is positively correlated with both AT ($r = 0.9079$, $P = 0.0123$) and PAG ($r = 0.8894$, $P = 0.0177$).

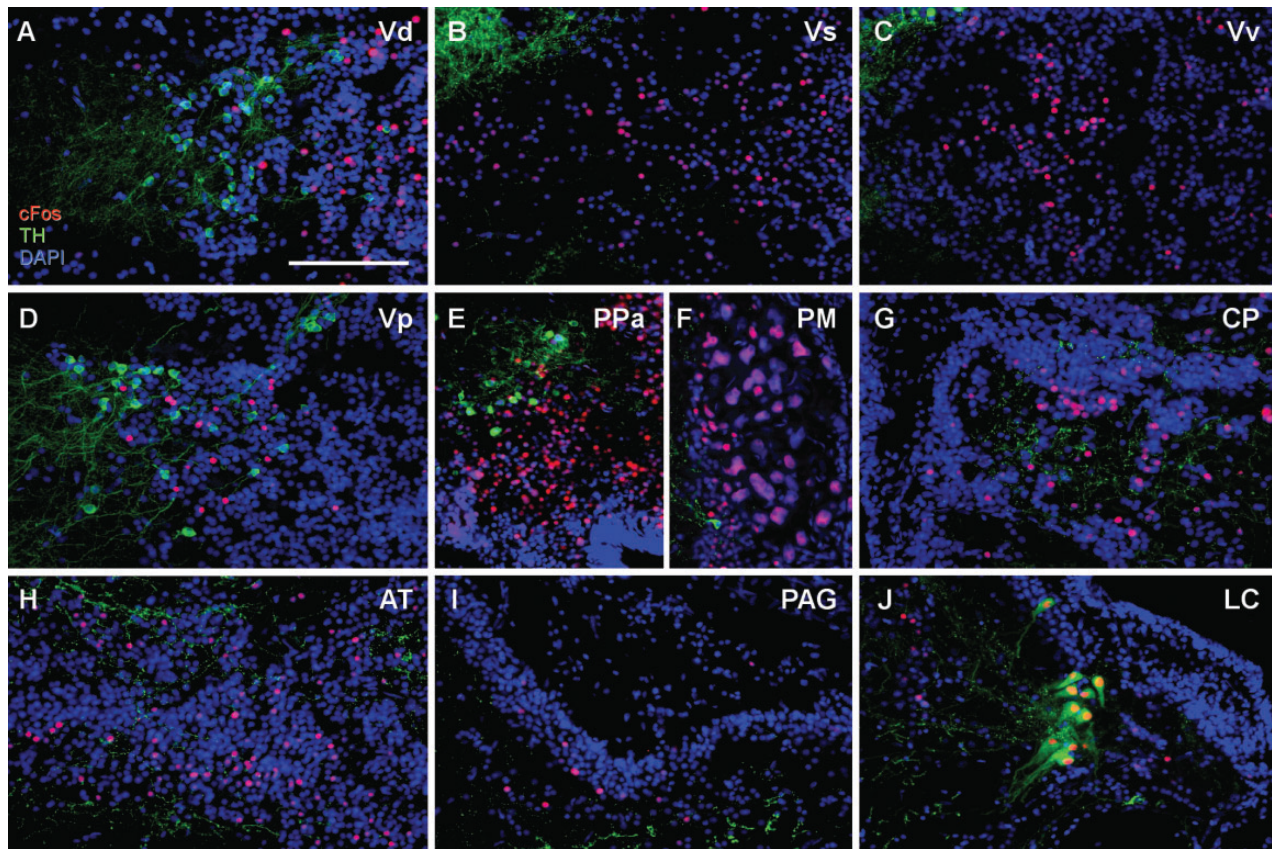


Fig. 2 Example micrographs showing nuclei found to have no significant relationship between time attending speaker and TH-ir + cFos colocalization (**A,D,E,J**) or cFos expression (**A-I**). Transverse sections are shown from the ventral telencephalon (V) (**A-D**): (**A**) dorsal nucleus of V (Vd), (**B**) supracommissural nucleus of V (Vs), (**C**) ventral nucleus of area V (Vv), and (**D**) postcommissural nucleus of area V (Vp). Diencephalon (**E-H**): (**E**) anterior parvocellular preoptic nucleus (PPa), (**F**) magnocellular preoptic nucleus (PM), (**G**) central posterior nucleus of the thalamus (CP), (**H**) anterior tuberal nucleus (AT). Brainstem (**I-J**): (**I**) periaqueductal gray (PAG), (**J**) locus coeruleus (LC). Scale bar = 100 μ m.

Negative correlations between nuclei

The number of negative correlations was mostly equivalent between responders and nonresponders (4 vs. 3) (Fig. 3, Suppl. Table 1). However, there were differences between groups with regard to which nuclei exhibited negative Pearson correlation coefficients. In responders, %TH + cFos-ir in PPa was negatively correlated with cFos-ir/section in PAG ($r = -0.5865$, $P = 0.045$), and %TH + cFos-ir in the NA-ergic LC was negatively correlated with cFos-ir/section in AT ($r = -0.7107$, $P = 0.0096$), which itself shared a negative relationship with Vp ($r = -0.6318$, $P = 0.0275$). In non-responders, %TH + cFos-ir in TPP shared negative relationships with cFos-ir/section in both Vd ($r = -0.8544$, $P = 0.0299$) and Vp ($r = -0.9533$, $P = 0.0467$). As mentioned above, the negative correlation between cFos-ir/section in Vp and Dm was shared in both groups of animals.

Discussion

The present study utilized phonotaxis behavior as an unambiguous measure of female sexual motivation (Forlano and Bass 2011). Similar to conspecific vocalizations in songbirds, the simple fundamental frequency playback of a hum can be viewed as signal with high incentive salience (see Maney 2013) as it is well documented to be necessary and sufficient to produce phonotaxis in gravid female midshipman (McKibben and Bass 1998; Bass and McKibben 2003; Zeddies et al. 2010). All females who responded to the male advertisement call made a decision to move toward and attend to the sound source for variable lengths of time. Therefore, all responders can be categorized as reproductively ready and the more time spent attending to the acoustic signal could reflect greater levels of arousal and motivation or drive for locating a mate. Harnessing individual female variability in duration

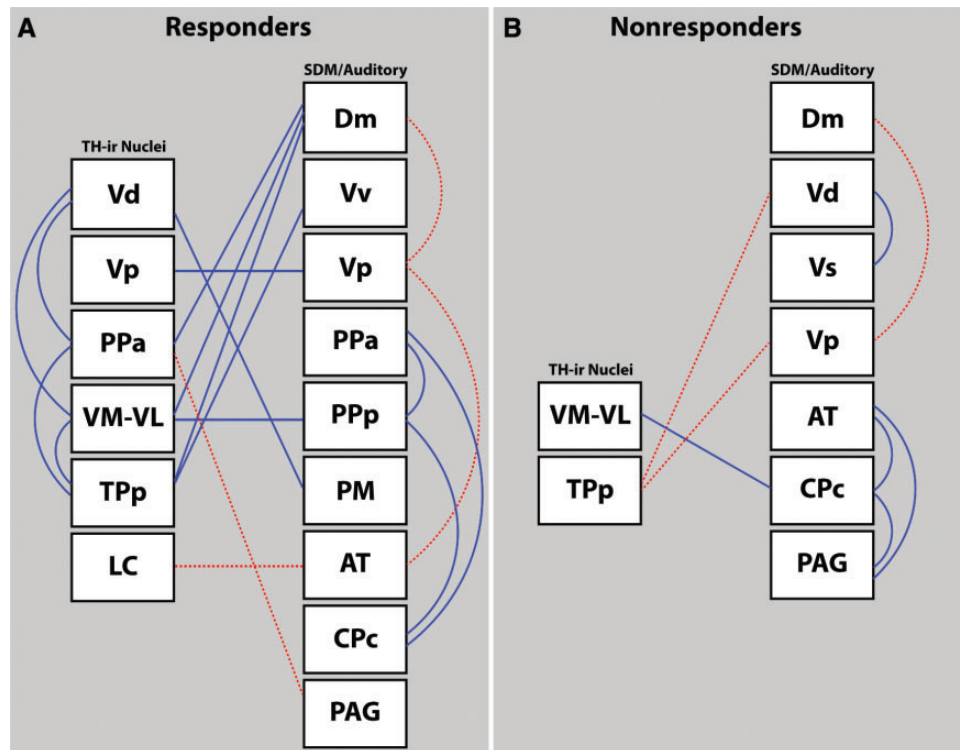


Fig. 3 Top-down schematic diagrams of correlated activity between catecholaminergic nuclei, social decision-making network (SDM) nodes, and auditory circuitry in responding (**A**) and nonresponding (**B**) females during playback of the male advertisement call. Positive Pearson coefficients (r -values) are represented as solid lines, and negative correlations are denoted with dotted lines. All correlations had P -values ≤ 0.0495 .

of the behavioral response to the playback, we sought to test which nuclei may co-vary and underlie variation in time attending the playback. Nonresponders, considered absolutely not motivated to respond to the playback call, were utilized as a baseline to compare the pattern of correlated brain activation to responders and create contrasting maps of brain coactivation in two divergent behavioral states (Fig. 3). Our results show that the cFos response in several forebrain nuclei (two of which are dopaminergic) are positively correlated to time attending to the reproductive acoustic stimulus. In addition, by comparing cFos coactivation across six catecholaminergic and ten SDM nuclei we can begin to identify functional neural networks underlying the coordination of auditory responsiveness with decision-making and subsequent motor responses to engage in reproductive behavior.

Results from the current study provide support for dopamine as a candidate neuromodulator underlying female sexual proceptivity in response to a social acoustic signal in midshipman. While a role for dopamine as a regulator of female sexual behavior and or neural response to male courtship signals is consistent with studies in other vertebrates (Mermelstein and Becker 1995; Ellingsen and

Agmo 2004; LeBlanc et al. 2007; Ritters et al. 2007; Maney et al. 2008; Matragrano et al. 2012), the main focus of dopamine in most other studies is known or proposed to originate in the midbrain VTA (A10), since it is a key element in the mesolimbic reward system (O'Connell and Hofmann 2011). Here we demonstrate both dopaminergic groups (TPp, VM-VL) responsive to time females attend to the playback reside in the diencephalon and have homologies to groups (A11, A13) not well studied in the context of social behavior (Yamamoto and Vernier 2011; Goodson and Kingsbury 2013). These results do, however, support dopaminergic TPp neurons as possibly serving functions analogous to VTA in mammals (Salamone and Correa 2012).

Nuclei with positive cFos-ir response in relation to time attending playback speaker

Two dopaminergic nuclei (VM-VL and TPp), a subdivision of the preoptic area, and the dorsomedial telencephalon were more active (contained greater numbers of cFos-ir cells) the longer the female was engaged in mate seeking behavior and are thus likely involved in maintaining the drive for mate seeking behavior. Therefore, females who persisted in this

behavior by attending to the playback speaker longer can be interpreted as being more motivated to find a mate. We believe it is highly unlikely that the cFos induction resulted merely from increased stimulus exposure because (1) we did not see a relationship between cFos and time attending to the playback in primarily auditory regions (e.g., AT, CPC), where one would expect IEG expression to positively correlate with stimulus exposure (e.g., Lu et al. 2009), and (2) nonresponders, who were also subjected to the stimulus for varying lengths of time showed no relationship of cFos induction and time of exposure to the playback.

The following discussion focuses, in part, on what is known about the above nuclei and why they are good candidates underlying auditory-driven appetitive reproductive behavior. As described above, dopaminergic TH-ir neurons in the TPP are ideal candidate neuromodulators of sensory-motor integration due to their projections to peripheral, hindbrain and thalamic auditory centers as well as ascending projections to limbic homologues in the ventral telencephalon and descending spinal innervation (Rink and Wullimann 2001; Tay et al. 2011; Forlano et al. 2014). While in zebrafish these neurons are demonstrated to be important for sensory and motor function (Lambert et al. 2012; Jay et al. 2015; Toro et al. 2015; Reinig et al. 2017), only in midshipman has a sensory input pathway onto these cells been delineated. Kittelberger and Bass (2013) demonstrated strong reciprocal connectivity between TPP and the PAG. Interestingly, the PAG receives ascending auditory input directly from hindbrain, midbrain (torus semicircularis), hypothalamic (AT) and thalamic (CP) nuclei (Goodson and Bass 2002; Kittelberger and Bass 2013). Indeed, playback exposure to field recorded hums elicits strong cFos-ir response in TPP TH-ir neurons in other midshipman males (Petersen et al. 2013). Thus, while these dopaminergic neurons are unlikely direct homologues to the tetrapod VTA (see Goodson and Kingsbury 2013), they may play a similarly important role in regulating behavioral responses to salient reproductive signals (O'Connell and Hofmann 2011, 2012; Forlano et al. 2014). In support of this, chemical lesioning of dopaminergic neurons in the posterior tuberculum of female green treefrogs caused a negative effect on phonotaxis behavior and is attributed to a degradation of motor processing and function (Endepols et al. 2004). Other immediate early gene studies in anurans suggest posterior tubercular dopamine neurons project to the striatum and are involved in sensory motor processing and important for phonotaxis (Hoke et al. 2007; Hoke and

Pitts 2012). Interestingly, systematic dopamine depletion in grey treefrogs produces a negative effect on attention to the courtship signal and suggests a role for dopamine in auditory filtering (Endepols et al. 2004). It is highly likely that due to the wide ranging projections of TPP neurons that vary with reproductive state, they play a complex role in both modulating auditory (peripheral and central) processing and coordinating locomotor response to reproductive social signals (Forlano et al. 2014; Forlano et al. 2015a; Perelmuter and Forlano 2017).

Unlike TH-ir neurons in the TPP, much less is known about the functional significance of dopaminergic neurons in the ventral thalamus (VM-VL) in fish and in other vertebrates in general. This group is most likely homologous to A13 incerto-hypothalamic projecting dopamine neurons in mammals (Yamamoto and Vernier 2011). In midshipman, TH-ir neurons in VM/VL appear to send prominent projections to the lateral division of nucleus preglomerulosus (PGL) (Forlano et al. 2014), a diencephalic auditory nucleus which receives input from the midbrain auditory torus semicircularis (Bass et al. 2000). A single study in zebra finches focused on the interactions of various dopaminergic nuclei on behavioral phenotype suggests A13 TH + cFos labeled neurons are important in the processing of social behavior, in particular social novelty, and a negative relationship to anxiety measures (Kelly and Goodson 2015). The current study is perhaps the first to provide evidence of these dopamine neurons involved in reproductive social behavior.

One subdivision of the preoptic area (PPp) showed a significant cFos response with time females attended to the playback. The preoptic area is perhaps one of the most well studied and conserved vertebrate brain regions known as a major neuroendocrine and sensory motor integration center controlling reproduction and homeostatic functions (Butler and Hodos 2005), and often thought of a functional unit with the anterior hypothalamus (see Forlano and Bass 2011 and refs within). In addition to the well characterized anatomical and neurochemical distinction of various POA subregions (Goodson et al. 2003; Bass and Grober 2009; Forlano and Bass 2011), the current study supports a functional separation of POA regions. Importantly, various tract-tracing studies have demonstrated the PPp receives input from the ascending auditory system (Bass et al. 2000; Goodson and Bass 2002; Forlano et al. 2014), and therefore sits in an ideal position to regulate behavioral output based on internal state (e.g., Maruska and Fernald 2011). Importantly, lesions to the preoptic area in anurans disrupt female

phonotaxis (Walkowiak et al. 1999). Furthermore, estradiol enhances the effect of hearing mate calls on the immediate early gene *egr-1* expression in the preoptic area of tungara frogs and may function as a hormonal mediator for phonotaxis (Chakraborty and Burmeister 2015).

Residing in the dorsomedial telencephalon, Dm is the proposed homologue to the ventral pallidum or laterobasal amygdala complex (Maximino et al. 2013; Table 1). It receives strong input, in part, from the auditory thalamus (CPc) (Goodson and Bass 2002) and may serve as the highest level of auditory processing in fishes (McCormick 2011). Importantly, targets of Dm projections include social behavior network nuclei such as ventral tuberal (vT, anterior hypothalamus), AT, and PPa, and Dm receives input from Ppp and PPa. Therefore, Dm sits as an important node in the SDM (O'Connell and Hofmann 2011, 2012) and likely regulates the highest form of auditory cognitive processing (integration of sensory input and decision-making and initiation of behavioral output) in teleosts. Previous lesioning studies in goldfish implicate Dm in emotional learning (Vargas et al. 2009). Immediate early gene induction in Dm has been investigated in zebrafish and an African cichlid and appears to be engaged in male-male social interactions (Maruska et al. 2013; Teles et al. 2015, 2016) as well as in female spawning behavior in medaka (Okuyama et al. 2011). The present study is the first to investigate the Dm in appetitive female reproductive behavior and corroborates known anatomical connections to auditory and SBN circuitry in midshipman.

Distinct brain coactivation patterns in female responders vs. non-responders

Correlation matrices were assembled to visualize coactivation of catecholamine nuclei, SBN/SDM nodes and the auditory thalamus (CPc) to generate putative functional relationships of circuitry underlying sexually motivated (responders) compared to unmotivated (non-responders) females. Even though all females could be categorized as reproductive since all females in the study were identified as "gravid" (GSI > 10%), not all females exhibited phonotaxis, indicating there is individual variability in female responsiveness to playbacks (see McKibben and Bass 1998; Zeddies et al. 2010). This is similar to studies on female starlings in the breeding season where there can be large individual variation in behavior that signals reproductive readiness (Pawlish et al. 2012). The differences in number of brain activation correlations between responders (18) and nonresponders (8)

(Fig. 3) may reflect functional connectivity patterns in these two divergent behavioral states. Interestingly, all six CA nuclei exhibited interactions with SBN/SDM nuclei in responders vs. just two in non-responders. Secondly, all preoptic area subdivisions exhibited some coactivation with other nuclei in responders but none were represented in non-responders. This striking difference between two behavioral states supports the preoptic area as fundamental to female appetitive reproductive behaviors.

Negative relationships could be explained in part by GABAergic nuclei within the SDM (Filippi et al. 2014; Mueller and Guo 2009; Maruska et al. 2017; Timothy and Forlano, unpublished observations). Also worth noting is that AT was the only nucleus that showed significant negative relationships between cFos-ir/section in Vp and %TH + cFos-ir in LC, indicating potential functional connectivity between these three brain regions. Goodson and Bass (2002) demonstrated that iontophoretic injections into the AT of midshipman resulted in putative terminals ventral to Vp near the anterior commissure in the forebrain. Additionally, it has been shown that 10–20% of noradrenergic neurons in LC project to the hypothalamus in developing zebrafish (Tay et al. 2011). Negative Pearson coefficients suggest that increased activity in AT may attenuate the phasic responses of LC ($r = -0.719$, $P = 0.014$) and Vp ($r = -0.64$, $P = 0.0339$), thereby serving as a possible negative relay through which noradrenergic activity in the hindbrain is conveyed to higher decision-making areas in the forebrain.

Tpp connectivity to ventral telencephalic nuclei (Vv/Vd) was initially established in zebrafish and supported evidence for the ascending dopaminergic system in teleosts originating in the Tpp (Rink and Wullimann 2001). Interestingly, the positive correlation in responders of Tpp- Vv (septal homologue; Goodson 2005; Goodson and Kingsbury 2013) contrasts with Tpp negatively correlated to Vd (striatal homologue) in nonresponders. This is consistent with studies in anurans showing septal and striatal lesions disrupt phonotaxis (Walkowiak et al. 1999).

Conclusions

The plainfin midshipman is becoming an emerging comparative model to investigate how various dopaminergic, and proposed SBN and SDM network nuclei interact to mediate appropriate behavioral responses to social acoustic cues. As a comparative model the midshipman is exemplified by its wealth of neural tract tracing studies that preceded and became the foundation for proposing the

reciprocally-connected SBN nuclei as a conserved vertebrate feature (Goodson 2005). Thus, many of the examples of neural coactivation using cFos as a marker for neural activity in the present study corroborate and complement preexisting neuroanatomical studies (e.g., Dm-Vp, Vp-AT, CPC-AT, CP-PPp/PPa, CP-PAG, AT-PAG; see Bass et al. 2000; Goodson and Bass 2002; Kittelberger and Bass 2013). Future studies of the midshipman should provide a strong neuroethological framework to test a number of hypotheses that could provide insight into the SDM and SBN components that are active during socially motivated behaviors.

Funding

This work was supported by the National Institutes of Health [SC2DA034996 to P.M.F.] and the National Science Foundation [IOS-1456743 to P.M.F. and IOS-1456700 to J.A.S.].

Acknowledgments

We thank Gary Cherr, Kitty Brown, and the UC Davis Bodega Marine Laboratory for logistical support, Alena Chernenko for histological assistance, Caitlin Cherry, Phoo Kyaw, Alex Dean for assistance with image analyses. We thank Jonathan Perelmuter and two anonymous reviewers for comments that improved the manuscript and Jim Goodson for his inspiration and early discussions about this study.

Supplementary data

Supplementary data available at *ICB* online.

References

- Bass AH. 1996. Shaping brain sexuality. *Am Sci* 84:352–63.
- Bass AH, Bodnar DA, Marchaterre MA. 2000. Midbrain acoustic circuitry in a vocalizing fish. *J Comp Neurol* 419:505–31.
- Bass AH, Gilland EH, Baker R. 2008. Evolutionary origins for social vocalization in a vertebrate hindbrain-spinal compartment. *Science (New York, NY)* 321:417–21.
- Bass AH, Grober MS. 2009. Reproductive plasticity in fish: evolutionary lability in the patterning of neuroendocrine and behavioral traits underlying divergent sexual phenotypes. In: Pfaff D, Arnold A, Etgen A, Rubin R, Fahrbach S, editors. *Hormones, brain, and behavior*. New York (NY): Academic Press.
- Bass AH, McKibben JR. 2003. Neural mechanisms and behaviors for acoustic communication in teleost fish. *Prog Neurobiol* 69:1–26.
- Bharati IS, Goodson JL. 2006. Fos responses of dopamine neurons to sociosexual stimuli in male zebra finches. *Neuroscience* 143:661–70.
- Braford MR Jr. 1995. Comparative aspects of forebrain organization in the ray-finned fishes: touchstones or not? *Brain Behav Evol* 46:259–74.
- Braford MR Jr, Northcutt RG. 1983. Organization of the diencephalon and pretectum of the ray-finned fishes. In: Davis RE and Northcutt RG, editors. *Fish neurobiology*. Ann Arbor (MI): University of Michigan Press. p. 117–64.
- Brantley RK, Bass AH. 1988. Cholinergic neurons in the brain of a teleost fish (*Porichthys notatus*) located with a monoclonal antibody to choline acetyltransferase. *J Comp Neurol* 275:87–105.
- Brantley RK, Bass AH. 1994. Alternative male spawning tactics and acoustic-signals in the plainfin midshipman fish *Porichthys notatus* Girard (*Teleostei, Batrachoididae*). *Ethology* 96:213–32.
- Bruce LL, Braford MR. 2009. Evolution of the limbic system. In: Squire LR, editor. *Encyclopedia of neuroscience*. Vol. 4. Oxford: Academic Press. p. 43–55.
- Butler AB, Hodos W. 2005. *Comparative vertebrate neuroanatomy: evolution and adaptation*. 2nd ed. Hoboken (NJ): John Wiley.
- Butler JM, Maruska KP. 2016. The mechanosensory lateral line system mediates activation of socially-relevant brain regions during territorial interactions. *Front Behav Neurosci* 10:93.
- Caras ML. 2013. Estrogenic modulation of auditory processing: a vertebrate comparison. *Front Neuroendocrinol* 34:285–99.
- Chakraborty M, Burmeister SS. 2015. Effects of estradiol on neural responses to social signals in female túngara frogs. *J Experimental Biol* 218:3671–7.
- Ellingsen E, Agmo A. 2004. Sexual-incentive motivation and paced sexual behavior in female rats after treatment with drugs modifying dopaminergic neurotransmission. *Pharmacol Biochem Behav* 77:431–45.
- Endepols H, Schul J, Gerhardt HC, Walkowiak W. 2004. 6-hydroxydopamine lesions in anuran amphibians: a new model system for Parkinson's disease? *J Neurobiol* 60:395–410.
- Filippi A, Mueller T, Driever W. 2014. vglut2 and gad expression reveal distinct patterns of dual GABAergic versus glutamatergic cotransmitter phenotypes of dopaminergic and noradrenergic neurons in the zebrafish brain. *J Comp Neurol* 522:2019–37.
- Forlano PM, Bass AH. 2011. Neural and hormonal mechanisms of reproductive-related arousal in fishes. *Horm Behav* 59:616–29.
- Forlano PM, Cone RD. 2007. Conserved neurochemical pathways involved in hypothalamic control of energy homeostasis. *J Comp Neurol* 505:235–48.
- Forlano PM, Deitcher DL, Bass AH. 2005. Distribution of estrogen receptor alpha mRNA in the brain and inner ear of a vocal fish with comparisons to sites of aromatase expression. *J Comp Neurol* 483:91–113.
- Forlano PM, Ghahramani ZN, Monestime CM, Kurochkin P, Chernenko A, Milkis D. 2015a. Catecholaminergic innervation of central and peripheral auditory circuitry varies with reproductive state in female midshipman fish, *Porichthys notatus*. *PLoS One* 10:e0121914.
- Forlano PM, Kim SD, Krzyminska ZM, Sisneros JA. 2014. Catecholaminergic connectivity to the inner ear, central auditory, and vocal motor circuitry in the plainfin

- midshipman fish *Porichthys notatus*. *J Comparative Neurol* 522:2887–927.
- Forlano PM, Sisneros JA. 2016. Neuroanatomical evidence for catecholamines as modulators of audition and acoustic behavior in a vocal teleost. *Adv Exp Med Biol* 877:439–75.
- Forlano PM, Sisneros JA, Rohmann KN, Bass AH. 2015b. Neuroendocrine control of seasonal plasticity in the auditory and vocal systems of fish. *Front Neuroendocrinol* 37:129–45.
- Ghahramani ZN, Timothy M, Kaur G, Gorbonosov M, Chernenko A, Forlano PM. 2015. Catecholaminergic fiber innervation of the vocal motor system is intrasexually dimorphic in a teleost with alternative reproductive tactics. *Brain Behav Evol* 86:131–44.
- Gilchrist BJ, Tipping DR, Hake L, Levy A, Baker BI. 2000. The effects of acute and chronic stresses on vasotocin gene transcripts in the brain of the rainbow trout (*Oncorhynchus mykiss*). *J Neuroendocrinol* 12:795–801.
- Goodson JL. 2005. The vertebrate social behavior network: evolutionary themes and variations. *Horm Behav* 48:11–22.
- Goodson JL, Bass AH. 2002. Vocal-acoustic circuitry and descending vocal pathways in teleost fish: convergence with terrestrial vertebrates reveals conserved traits. *J Comp Neurol* 448:298–322.
- Goodson JL, Evans AK, Bass AH. 2003. Putative isotocin distributions in sonic fish: relation to vasotocin and vocal-acoustic circuitry. *J Comp Neurol* 462:1–14.
- Goodson JL, Kabelik D. 2009. Dynamic limbic networks and social diversity in vertebrates: from neural context to neuro-modulatory patterning. *Front Neuroendocrinol* 30:429–41.
- Goodson JL, Kingsbury MA. 2013. What's in a name? Considerations of homologies and nomenclature for vertebrate social behavior networks. *Horm Behav* 64:103–12.
- Graham MD, Pfaus JG. 2012. Differential effects of dopamine antagonists infused to the medial preoptic area on the sexual behavior of female rats primed with estrogen and progesterone. *Pharmacol Biochem Behav* 102:532–9.
- Hoke KL, Pitts NL. 2012. Modulation of sensory-motor integration as a general mechanism for context dependence of behavior. *Gen Comp Endocrinol* 176:465–71.
- Hoke KL, Ryan MJ, Wilczynski W. 2007. Functional coupling between substantia nigra and basal ganglia homologues in amphibians. *Behav Neurosci* 121:1393–9.
- Jay M, De Faveri F, McDearmid JR. 2015. Firing dynamics and modulatory actions of supraspinal dopaminergic neurons during zebrafish locomotor behavior. *Curr Biol* 25:435–44.
- Kapsimali M, Bourrat F, Vernier P. 2001. Distribution of the orphan nuclear receptor Nurr1 in medaka (*Oryzias latipes*): cues to the definition of homologous cell groups in the vertebrate brain. *J Comp Neurol* 431:276–92.
- Kelly AM, Goodson JL. 2015. Functional interactions of dopamine cell groups reflect personality, sex, and social context in highly social finches. *Behav Brain Res* 280:101–12.
- Kittelberger JM, Bass AH. 2013. Vocal-motor and auditory connectivity of the midbrain periaqueductal gray in a teleost fish. *J Comp Neurol* 521:791–812.
- Lambert AM, Bonkowsky JL, Masino MA. 2012. The conserved dopaminergic diencephalospinal tract mediates vertebrate locomotor development in zebrafish larvae. *J Neurosci* 32:13488–500.
- LeBlanc MM, Goode CT, MacDougall-Shackleton EA, Maney DL. 2007. Estradiol modulates brainstem catecholaminergic cell groups and projections to the auditory forebrain in a female songbird. *Brain Res* 1171:93–103.
- Lu H-P, Chen S-T, Poon PW-F. 2009. Nuclear size of c-Fos expression at the auditory brainstem is related to the time-varying nature of the acoustic stimuli. *Neurosci Lett* 451:139–43.
- Maney DL, Goode CT, Lange HS, Sanford SE, Solomon BL. 2008. Estradiol modulates neural responses to song in a seasonal songbird. *J Comp Neurol* 511:173–86.
- Maney DL. 2013. The incentive salience of courtship vocalizations: hormone-mediated “wanting” in the auditory system. *Hear Res* 305:19–30.
- Maney DL, Rodriguez-Saltos CA. 2016. Hormones and the incentive salience of bird song. In: Bass AH, Sisneros JA, Popper AN, Fay, RR, editors. *Hearing and hormones*. New York (NY): Springer International Publishing. p. 101–32.
- Maruska KP, Fernald RD. 2011. Social regulation of gene expression in the hypothalamic-pituitary-gonadal axis. *Physiology (Bethesda)* 26:412–23.
- Maruska KP, Zhang A, Neboori A, Fernald RD. 2013. Social opportunity causes rapid transcriptional changes in the social behaviour network of the brain in an African cichlid fish. *J Neuroendocrinol* 25:145–57.
- Maruska KP, Butler JM, Field KE, Porter DT. 2017. Localization of glutamatergic, GABAergic, and cholinergic neurons in the brain of the African cichlid fish, *Astatotilapia burtoni*. *J Comp Neurol* 525:610–38.
- Matragrano LL, Beaulieu M, Phillip JO, Rae AI, Sanford SE, Sockman KW, Maney DL. 2012. Rapid effects of hearing song on catecholaminergic activity in the songbird auditory pathway. *PLoS One* 7:e39388.
- Maximino C, Lima MG, Oliveira KR, Batista Ede J, Herculano AM. 2013. “Limbic associative” and “autonomic” amygdala in teleosts: a review of the evidence. *J Chem Neuroanat* 48–49:1–13.
- McCormick CA. 2011. Auditory/lateral line CNS: anatomy. In: Farrell AP, editor. *Encyclopedia of fish physiology: from genome to environment*. San Diego (CA): Academic Press. p. 283–91.
- McHenry JA, Otis JM, Rossi MA, Robinson JE, Kosyk O, Miller NW, McElligott ZA, Budygin EA, Rubinow DR, Stuber GD. 2017. Hormonal gain control of a medial preoptic area social reward circuit. *Nat Neurosci* 20:449–58.
- McKibben JR, Bass AH. 1998. Behavioral assessment of acoustic parameters relevant to signal recognition and preference in a vocal fish. *J Acoust Soc Am* 104:3520–33.
- Mermelstein PG, Becker JB. 1995. Increased extracellular dopamine in the nucleus accumbens and striatum of the female rat during paced copulatory behavior. *Behav Neurosci* 109:354–65.
- Moore FL, Lowry CA. 1998. Comparative neuroanatomy of vasotocin and vasopressin in amphibians and other vertebrates. *Comp Biochem Physiol C Pharmacol Toxicol Endocrinol* 119:251–60.
- Mueller T. 2012. What is the thalamus in zebrafish? *Front Neurosci* 6:64.

- Mueller T, Guo S. 2009. The distribution of GAD67-mRNA in the adult zebrafish (teleost) forebrain reveals a prosomeric pattern and suggests previously unidentified homologies to tetrapods. *J Comp Neurol* 516:553–68.
- Mueller T, Wullimann MF. 2009. An evolutionary interpretation of teleostean forebrain anatomy. *Brain Behav Evol* 74:30–42.
- Newman SW. 1999. The medial extended amygdala in male reproductive behavior. A node in the mammalian social behavior network. *Ann N Y Acad Sci* 877:242–57.
- Northcutt RG. 1995. The forebrain of gnathostomes: in search of a morphotype. *Brain Behav Evol* 46:275–318.
- Northcutt RG. 2006. Connections of the lateral and medial divisions of the goldfish telencephalic pallium. *J Comp Neurol* 494:903–43.
- O'Connell LA, Hofmann HA. 2011. The vertebrate mesolimbic reward system and social behavior network: a comparative synthesis. *J Comp Neurol* 519:3599–639.
- O'Connell LA, Hofmann HA. 2012. Evolution of a vertebrate social decision-making network. *Science* 336:1154–7.
- O'Connell LA, Rigney MM, Dykstra DW, Hofmann HA. 2013. Neuroendocrine mechanisms underlying sensory integration of social signals. *J Neuroendocrinol* 25:644–54.
- Okuyama T, Suehiro Y, Imada H, Shimada A, Naruse K, Takeda H, Kubo T, Takeuchi H. 2011. Induction of *c-fos* transcription in the medaka brain (*Oryzias latipes*) in response to mating stimuli. *Biochem Biophys Res Commun* 404:453–7.
- Pawlish BA, Kelm-Nelson CA, Stevenson SA, Ritters LV. 2012. Behavioral indices of breeding readiness in female European starlings correlate with immunolabeling for catecholamine markers in brain areas involved in sexual motivation. *Gen Comp Endocrinol* 179:359–68.
- Petersen CL, Timothy M, Kim DS, Bhandiwad AA, Mohr RA, Sisneros JA, Forlano PM. 2013. Exposure to advertisement calls of reproductive competitors activates vocal-acoustic and catecholaminergic neurons in the plainfin midshipman fish, *Porichthys notatus*. *PLoS One* 8:e70474.
- Perlmutter JT, Forlano PM. 2017. Connectivity and ultrastructure of dopaminergic innervation of the inner ear and auditory efferent system of a vocal fish. *J Comp Neurol* 525:2090–108.
- Portavella M, Torres B, Salas C. 2004. Avoidance response in goldfish: emotional and temporal involvement of medial and lateral *Telencephalic pallium*. *J Neurosci* 24:2335–42.
- Reinig S, Driever W, Arrenberg AB. 2017. The descending diencephalic dopamine system is tuned to sensory stimuli. *Curr Biol* 27:318–33.
- Rink E, Wullimann MF. 2001. The teleostean (zebrafish) dopaminergic system ascending to the subpallium (striatum) is located in the basal diencephalon (posterior tuberculum). *Brain Res* 889:316–30.
- Ritters LV, Olesen KM, Auger CJ. 2007. Evidence that female endocrine state influences catecholamine responses to male courtship song in European starlings. *Gen Comp Endocrinol* 154:137–49.
- Salamone JD, Correa M. 2012. The mysterious motivational functions of mesolimbic dopamine. *Neuron* 76:470–85.
- Schweitzer J, Lohr H, Filippi A, Driever W. 2012. Dopaminergic and noradrenergic circuit development in zebrafish. *Dev Neurobiol* 72:256–68.
- Smeets WJ, Gonzalez A. 2000. Catecholamine systems in the brain of vertebrates: new perspectives through a comparative approach. *Brain Res Brain Res Rev* 33:308–79.
- Sisneros JA. 2009. Steroid-dependent auditory plasticity for the enhancement of acoustic communication: recent insights from a vocal teleost fish. *Hear Res* 252:9–14.
- Sisneros JA, Forlano PM, Deitcher DL, Bass AH. 2004a. Steroid-dependent auditory plasticity leads to adaptive coupling of sender and receiver. *Science* 305:404–7.
- Sisneros JA, Forlano PM, Knapp R, Bass AH. 2004b. Seasonal variation of steroid hormone levels in an intertidal-nesting fish, the vocal plainfin midshipman. *Gen Comp Endocrinol* 136:101–16.
- Tay TL, Ronneberger O, Ryu S, Nitschke R, Driever W. 2011. Comprehensive catecholaminergic projectome analysis reveals single-neuron integration of zebrafish ascending and descending dopaminergic systems. *Nat Commun* 2:171.
- Teles MC, Cardoso SD, Oliveira RF. 2016. Social plasticity relies on different neuroplasticity mechanisms across the brain social decision-making network in zebrafish. *Front Behav Neurosci* 10:16.
- Teles MC, Almeida O, Lopes JS, Oliveira RF. 2015. Social interactions elicit rapid shifts in functional connectivity in the social decision-making network of zebrafish. *Proc Biol Sci* 282:20151099.
- Toro C, Trapani JG, Pacentine I, Maeda R, Sheets L, Mo W, Nicolson T. 2015. Dopamine modulates the activity of sensory hair cells. *J Neurosci* 35:16494–503.
- Vargas JP, Lopez JC, Portavella M. 2009. What are the functions of fish brain pallium? *Brain Res Bull* 79:436–40.
- Von Trotha JW, Vernier P, Bally-Cuif L. 2014. Emotions and motivated behavior converge on an amygdala-like structure in the zebrafish. *Eur J Neurosci* 40:3302–15.
- Walkowiak W, Berlinger M, Schul J, Gerhardt HC. 1999. Significance of forebrain structures in acoustically guided behavior in anurans. *Eur J Morphol* 37:177–81.
- Wilczynski W, Ryan MJ. 2010. The behavioral neuroscience of anuran social signal processing. *Curr Opin Neurobiol* 20:754–63.
- Wullimann MF, Mueller T. 2004. Teleostean and mammalian forebrains contrasted: evidence from genes to behavior. *J Comp Neurol* 475:143–62.
- Yamamoto K, Vernier P. 2011. The evolution of dopamine systems in chordates. *Front Neuroanat* 5:21.
- Zeddies DG, Fay RR, Alderks PW, Shaub KS, Sisneros JA. 2010. Sound source localization by the plainfin midshipman fish, *Porichthys notatus*. *J Acoust Soc Am* 127:3104–13.